

Wireless Powered Sensor Networks for Internet of Things: Maximum Throughput and Optimal Power Allocation

Zheng Chu, *Member, IEEE*, Fuhui Zhou, *Member, IEEE*, Zhengyu Zhu, *Member, IEEE*
Rose Qingyang Hu, *Senior Member, IEEE*, Pei Xiao, *Senior Member, IEEE*

Abstract—This paper investigates a wireless powered sensor network (WPSN), where multiple sensor nodes are deployed to monitor a certain external environment. A multi-antenna power station (PS) provides the power to these sensor nodes during wireless energy transfer (WET) phase, and consequently the sensor nodes employ the harvested energy to transmit their own monitoring information to a fusion center (FC) during wireless information transfer (WIT) phase. The goal is to maximize the system sum throughput of the sensor network, where two different scenarios are considered, i.e., PS and the sensor nodes belong to the same or different service operator(s). For the first scenario, we propose a global optimal solution to jointly design the energy beamforming and time allocation. We further develop a closed-form solution for the proposed sum throughput maximization. For the second scenario in which the PS and the sensor nodes belong to different service operators, energy incentives are required for the PS to assist the sensor network. Specifically, the sensor network needs to pay in order to purchase the energy services released from the PS to support WIT. In this case, the paper exploits this hierarchical energy interaction, which is known as *energy trading*. We propose a *quadratic energy trading based Stackelberg game*, *linear energy trading based Stackelberg game*, and *social welfare* scheme, in which we derive the *Stackelberg* equilibrium for the formulated games, and the optimal solution for the *social welfare* scheme. Finally, numerical results are provided to validate the performance of our proposed schemes.

Index Terms—Wireless powered sensor networks, sum throughput maximization, energy trading, *Stackelberg* game, social welfare

I. INTRODUCTION

In recent years, wireless sensor networks (WSNs) have been considered as one of the thriving technologies with the advance of internet of things (IoT) [1]. WSNs have wide range of applications, from environment monitoring, i.e., pollution prevention, precision agriculture, structures and buildings health, to event detection, i.e., intrusions, fire/flood emergencies, and target tracking, i.e., surveillance [2]. A WSN is composed of a large number of sensor nodes for data

monitoring and a fusion center to process the data sent from these sensor nodes. Traditionally, batteries or other embedded energy sources are fixed to provide energy for these sensor nodes in WSNs [3]. The short battery life limits their potential applications in practice. Although the battery lifetime can be extended by periodically replacing or recharging the batteries, it may be difficult, costly, dangerous, or even impossible in many applications due to the fact that the sensors can be located inside toxic environments, building structures, or human bodies [4]. Although there have been many efforts in power management policies, the sensor nodes' lifetime still remains a performance bottleneck and makes the wide-range deployment of WSNs challenging.

In order to address the energy-constrained issue, radio frequency (RF) energy harvesting (EH) as one of the promising techniques, has received much attention, since it can provide unlimited power to the sensor nodes which scavenge energy from the environment (i.e., solar, wind, etc.) [5], [6]. Among these, RF energy radiated by ambient transmitters is almost ubiquitous [7], which can be harvested more effectively from wireless RF signals. Since RF signal can carry energy and information simultaneously, energy harvesting (EH) and simultaneous wireless information and power transfer (SWIPT) [8]–[10] is becoming a more and more promising research direction.

With recent advance of RF EH and SWIPT, wireless powered communication networks (WPCNs) has become a new wireless networking technology, where wireless devices (WDs) can be remotely powered by RF wireless energy transfer (WET) [7], [11]. Devices in a WPCN are charged by a dedicated wireless energy source [7], [11]. In addition, the energy released by the energy source is adjustable to satisfy different physical conditions and service criterion [7], [12]. With the development of WPCNs, a well-known protocol “*harvest-then-transmit*” was proposed in [13], where wireless users harvest energy from the RF signals broadcasted by a hybrid access-point (AP) in the downlink (DL). They further use the harvested energy to send their own information to the AP in uplink (UL). Recently, a dedicated wireless energy transfer (WET) network was proposed to deploy multiple power stations (PSs) near wireless information transfer (WIT) network, where these PSs provide wireless energy services to user terminals via RF signals [14], [15]. In [16], wireless powered relays have been investigated in full-duplex two-way communication to utilize the harvested energy from the access

Z. Chu and P. Xiao are with the 5G Innovation Center, Institute of Communication Systems, University of Surrey, Guildford, GU2 7XH, United Kingdom. (Email: zheng.chu@surrey.ac.uk; p.xiao@surrey.ac.uk)

F. Zhou and Q. Hu are with the Department of Electrical and Computer Engineering, Utah State University, Logan, UT, USA. F. Zhou is also with the School of Information Engineering and Post-Doctoral Research Station of Environmental Science and Engineering, Nanchang University, Nanchang 330031, China. (Email: zhoufuhui1989@163.com; rose.hu@usu.edu)

Z. Zhu is with the School of Information Engineering, Zhengzhou University, Zhengzhou, China. (Email: zhuzhengyu6@gmail.com).

points (APs) and self-interference (SI) to transmit information signal. Compared to SWIPT networks, WPCNs have a lower implementation cost since implementing WET networks is rather simple. Thus it is feasible to deploy PSs densely to ensure a good coverage without the need for backhaul links [17].

One of the potential applications of WPCN is the radio frequency identification (RFID) system that usually consists of a reader and many tags [11]. Specifically, a reader provides the RF energy to the energy-constrained tags, and the tags transmit their identification data to the reader via one-hop backscatter communication using the harvested RF energy. Backscatter communication is to efficiently reduce the power consumption. However, this type of RFID system is restricted to the short-range communications only. With the advances of ultra low-power electronics and RF EH technologies, it is feasible to envisage more sophisticated RFID-like devices that are able to not only harvest RF energy, but also conduct sensing, processing and active communication [18].

In order to circumvent the energy-constrained issue of WSNs, wireless-powered WSNs is considered in the recent work [19]–[21]. In [19], multi-antenna WPSN is investigated, in which a PS transfers electric energy to a sensor node via an electromagnetic wave, and a real-life multi-antenna WPSN testbed was built to conduct extensive experiments. The work in [20] proposed the power allocation and beam selection for distributed estimation in wireless passive sensor networks, where the sensors are charged by RF energy sources. [21] studied power allocation for distributed estimation in WSNs with a multiple-antenna fusion center (FC) and an unknown scalar random source, in which the sensor nodes are equipped with RF-based EH technology. Observation from sensor nodes is locally processed by using an uncoded amplify-and-forward (AF) scheme. The processed signals are sent to the FC and are coherently combined at the FC, where the best linear unbiased estimator (BLUE) is adopted for reliable estimation [21]. To incorporate this imperfect CSI, the robust design is considered in existing channel uncertainty model [22], where the authors investigated the physical layer security problem in relay WSNs with SWIPT by incorporating a spherical channel uncertainty model.

The deployment of a dedicated WET network in the existing WIT network was investigated in [14], where the updated network provides both wireless access and energy services. By considering quality-of-service (QoS) constraints on data links, a tradeoff between the densities of base stations and that of PSs was quantified by modeling the network using stochastic geometry theory [14]. Note that it is assumed in [14] that the WET network is deployed by the same service provider as the existing network. However, in practice, WET and WIT networks can be deployed by different service providers¹. In such situations, energy incentives (e.g., monetary payments) are needed for the WET network to provide wireless charging services to the WIT network. Here, we call the demand and

provision of the energy services as *energy trading* between WET and WIT networks. To the best of our knowledge, there have been no published works that model and investigate this hierarchical energy interaction in WPSN. This knowledge gap has motivated our research in this paper.

In this paper, we consider a WPSN that consists of a multi-antenna PS belonging to the WET network, multiple wireless sensor nodes and a FC belonging to the WIT network. Based on this system model, major contributions of this paper are highlighted in the following:

- 1) *Cooperation based sum throughput optimization*: First, we consider an ideal case in which both PS and the sensor network belong to the same service provider. The PS and the sensor network work together to maximize the mutual benefits and to formulate the sum throughput maximization (STM) problem that jointly optimizes the time allocation and energy beamforming.
- 2) *Energy trading/social welfare based sum throughput optimization*: We further consider a more practical and challenging scenario in which the PS and the sensor network belong to different service providers. In this case, the hierarchical energy interaction (i.e., *energy trading*) between PS and the sensor network is exploited, where the energy incentives (i.e., monetary payments) are charged to the sensor network to purchase the energy services released from the PS.
 - a) We first consider the wireless charging model as a *quadratic energy trading* process to facilitate the derivation of the optimal power allocation policies for the PS and the sensor network. Specifically, we take into account strategic behaviors of the PS and the sensor network and formulate this energy trading process as a *Stackelberg* game.
 - b) As comparison, we further develop a linear energy trading based *Stackelberg* game, which adopts a linear energy cost model to exploit the hierarchical energy interaction between the PS and the sensor networks. We formulate this energy interaction as a *Stackelberg* game for a fixed energy transfer time allocation. We derive the *Stackelberg* equilibrium for the formulated game, where both optimal energy transfer price and the PS transmit power can be achieved by a closed-form solution.
 - c) We further formulate a social welfare optimization scheme in order to exploit the performance loss with the selfish behaviors in PS in *energy trading* based *Stackelberg* games. In this case, both PS and the sensor network cooperatively maximize a *social welfare*, i.e., the difference between the benefits obtained from the sum throughput at the sensor network and the energy transfer operation cost of the PS.

The rest of the paper is organized as follows. Section II presents the system model. Section III solves the sum throughput maximization problem for the WPSN, whereas the game theory based WPSN is investigated in Section IV. Section V provides simulation results to validate the theoretical deriva-

¹It is assumed that the WET service is provided by one service provider, e.g., an energy supplier, while the WIT service is provided by another service provider, e.g., a telecommunication supplier. Two service providers belong to different authorities.

tions. Finally, Section VI concludes the paper.

Notations: We use upper case boldface letters for matrices and lower case boldface letters for vectors. $(\cdot)^T$ and $(\cdot)^H$ denote the transpose and conjugate transpose, respectively. $\text{Tr}(\cdot)$ and $\mathbb{E}\{\cdot\}$ stand for trace of a matrix and the statistical expectation for random variables, respectively. $\lambda_{max}(\mathbf{A})$ represents the maximum eigenvalue of \mathbf{A} , whereas $\mathbf{v}_{max}(\mathbf{A})$ denotes the eigenvector associated with the maximum eigenvalue of \mathbf{A} . $\mathbf{A} \succeq 0$ indicates that \mathbf{A} is a positive semidefinite matrix. $[x]^+ = \max(x, 0)$. Finally, $|\cdot|$ and $\|\cdot\|$ represent the magnitude and Euclidean norm, respectively.

II. SYSTEM MODEL

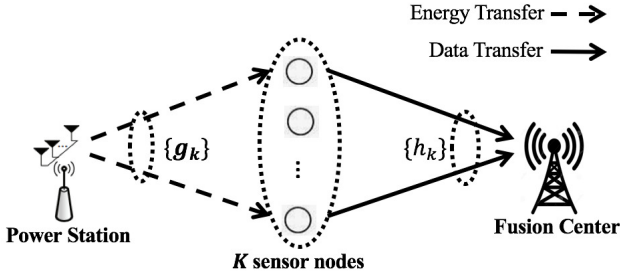


Fig. 1: System model consisting of a power station equipped with N_T transmit antennas, a single-antenna fusion center and K single-antenna sensor nodes.

We consider a WPSN, shown in Fig. 1, that consists of one PS² equipped with N_T transmit antennas, K single-antenna sensor nodes \mathcal{U}_k , $\forall k = 1, \dots, K$, and a single-antenna FC. The sensor nodes monitor the surrounding environments, e.g., temperature, pressure, humidity, or even emergency scenarios, and send their own monitoring data to the FC. It is assumed that all sensor nodes are only powered by harvested ambient RF energy provided by the PS and a *harvested-then-transmit* protocol is adopted in these sensor nodes. The PS first provides energy to those single-antenna sensor nodes. Then those sensor nodes employ “*harvest-then-transmit*” protocol to send their own information based on time division multiple access (TDMA) scheme to the single-antenna FC, which collects the monitoring data of the sensor nodes. It is assumed that the whole operation time period is T . During the downlink transmission duration $\theta_0 T$, $\theta_0 \in (0, 1)$, the PS employs an energy beamforming to broadcasts the wireless RF power to K sensor nodes. Further, during the uplink duration, each sensor node \mathcal{U}_k uses the harvested RF energy to send its own monitoring information in $\theta_k T$, $\theta_k \in [0, 1)$, to the FC one by one.³ Without loss of generality, it is assumed that $T = 1$ and thus we interchangeably use *power* and *energy* throughout the paper. Hence, the total time constraint can be written as $\sum_{k=0}^K \theta_k = 1$. Let $\mathbf{g}_k \in \mathbb{C}^{N_T}$ be the channel coefficients between the PS and the \mathcal{U}_k while $h_k \in \mathbb{C}$ be the

²The PS is powered constantly by a national grid or a micro grid, which means that it can serve as a stable energy source to provide energy to the sensor nodes.

³Note that $\theta_k = 0$, $\forall k$ holds if k -th sensor node is inactive and does not involve the data transmission, whereas $\theta_k \neq 1$ owing to the fact that each sensor node has to harvest energy during the $\theta_0 > 0$ time period.

channel coefficient between the FC and the \mathcal{U}_k . Let $\mathbf{w} \in \mathbb{C}^{N_T}$ ($\|\mathbf{w}\|^2 = 1$) be the normalized energy beamforming vector sent by the PS, the harvested energy at \mathcal{U}_k is

$$E_k = \xi_k \theta_0 P_B |\mathbf{g}_k^H \mathbf{w}|^2, \forall k, \quad (1)$$

where P_B is the maximum transmit power available at the PS and ξ_k denotes the EH efficiency at \mathcal{U}_k , for all k . Since all the harvested RF energy is used for the information transmission at sensor nodes, the transmit power p_k within θ_k time period can be written as

$$p_k = \frac{E_k}{\theta_k} = \frac{\xi_k \theta_0 P_B}{\theta_k} |\mathbf{g}_k^H \mathbf{w}|^2, \forall k. \quad (2)$$

Hence, the achievable throughput of sensor node \mathcal{U}_k can be expressed as

$$\begin{aligned} R_k(\theta, \mathbf{w}) &= \theta_k \log \left(1 + \frac{p_k |h_k|^2}{\sigma_k^2} \right) \\ &= \theta_k \log \left(1 + \frac{\theta_0 \xi_k P_B |\mathbf{g}_k^H \mathbf{w}|^2 |h_k|^2}{\sigma_k^2 \theta_k} \right), \forall k. \end{aligned} \quad (3)$$

$\theta = [\theta_0, \theta_1, \dots, \theta_K]^T$ and σ_k^2 denotes the variance of a zero mean circularly symmetric complex Gaussian noise at sensor node \mathcal{U}_k . Note that in our paper, it is assumed that each sensor node (i.e., \mathcal{U}_k , $\forall k$) consumes all the harvested energy during θ_0 time period to transmit its own information signal to the FC during its time allocation θ_k .

III. COOPERATIVE SUM THROUGHPUT OPTIMIZATION

In this section, we consider an ideal scenario where both PS and sensor nodes belong to the same service operator. Hence, they can cooperatively work to maximize their common benefits, i.e., system sum throughput. In the following, we propose a global optimal solution with a low complexity to jointly design the energy beamforming vector \mathbf{w} and time allocation duration θ .

A. Global Optimal Solution

In this subsection, we formulate the sum throughput maximization (STM) problem with semidefinite programming relaxation (SDR) (i.e., $\mathbf{W} = \mathbf{w}\mathbf{w}^H$) as

$$\begin{aligned} \max_{\theta, \mathbf{W}} \quad & \sum_{k=1}^K \theta_k \log \left(1 + \frac{t_k \theta_0 P_B}{\theta_k} \mathbf{g}_k^H \mathbf{W} \mathbf{g}_k \right), \\ \text{s.t.} \quad & \sum_{k=0}^K \theta_k \leq 1, \theta_k \geq 0, \forall k, \text{Tr}(\mathbf{W}) \leq 1, \mathbf{W} \succeq 0, \end{aligned} \quad (4)$$

where $t_k = \frac{\xi_k |h_k|^2}{\sigma_k^2}$. Letting $\mathbf{Q} = \theta_0 \mathbf{W}$, (4) can be equivalently modified to

$$\begin{aligned} \max_{\theta, \mathbf{Q}} \quad & \sum_{k=1}^K \theta_k \log \left(1 + \frac{t_k P_B}{\theta_k} \text{Tr}(\mathbf{g}_k \mathbf{g}_k^H \mathbf{Q}) \right), \\ \text{s.t.} \quad & \sum_{k=0}^K \theta_k \leq 1, \end{aligned} \quad (5a)$$

$$\theta_k \geq 0, \forall k, \quad (5b)$$

$$\text{Tr}(\mathbf{Q}) \leq \theta_0, \mathbf{Q} \succeq 0.$$

The problem formulated in (5) can be proved to be a convex optimization problem. First, the objective function in (5) is

the sum of concave function.⁴ Hence, the objective function is a concave function. In addition, all the constraints in (5) are linear and thus are convex constraints [23], [24]. Therefore, (5) is a convex optimization problem. Note that we have relaxed rank-one constraints on \mathbf{W} and \mathbf{Q} in (4) and (5), respectively. To that end, we introduce the following lemma.

Lemma 1: The optimal solutions to (4) and (5), i.e., \mathbf{W}^* and \mathbf{Q}^* , respectively, are rank-one matrices.

Proof: See Appendix A. ■

Since (5) is a convex optimization problem, it can be efficiently solved by using interior-point methods to obtain the global optimal solution [23]. Having the rank-one optimal solution \mathbf{W}^* , the optimal energy beamforming vector \mathbf{w}^* is obtained as the product of the eigenvector and eigenvalue of \mathbf{W}^* .

Although there are existing optimization packages, e.g., CVX, to solve convex optimization problem (5), it is desirable to develop an independent algorithm that can be deployed on the sensor nodes. To that end, we derive an optimal closed-form solution for (4) to reduce the computation complexity of global optimal solution in the following.

B. Closed-form Solution

In this section, we propose a new optimal closed-form solution to the problem in (5). We first derive the closed-form solution to θ_k , $\forall k$, which is written as a function with respect to θ_0 for a given \mathbf{Q} . Then, the optimal solutions to \mathbf{Q} and θ_0 are derived. To proceed, we consider the Lagrange dual function for a given \mathbf{Q} , as follows:

$$\mathcal{L}(\theta_k, \nu) = \sum_{k=1}^K \theta_k \log \left(1 + \frac{t_k P_B \text{Tr}(\mathbf{g}_k \mathbf{g}_k^H \mathbf{Q})}{\theta_k} \right) - \nu \left(\sum_{k=1}^K \theta_k - 1 + \theta_0 \right), \quad (6)$$

where ν is the non-negative Lagrange dual multipliers associated with constraints (5a). Thus, its associated dual problem is given as

$$\min_{\theta_k \in \mathcal{S}} \mathcal{L}(\theta_k, \nu), \forall k, \quad (7)$$

where \mathcal{S} is the feasible set of any θ_k , $\forall k$, and has been shown in the constraints (5a) and (5b). Note that the problem (5) is convex and satisfies Slater's condition, due to the fact that $\theta_k \in \mathcal{S}$, $\theta_k > 0$, for any k , with $\sum_{k=1}^K \theta_k < 1$. Thus, the strong duality holds such that the global optimal solution for (5) satisfies the Karush-Kuhn-Tucker (KKT) conditions, which is given by

$$\nu^* \left(\sum_{k=0}^K \theta_k^* - 1 \right) = 0, \quad (8a)$$

$$\frac{\partial \mathcal{L}}{\partial \theta_k} = 0. \quad (8b)$$

From (8a), it is verified that $\nu^* > 0$ since $\sum_{k=0}^K \theta_k^* = 1$ always holds for the problem (5). Thus, according to (8b), we

⁴Each term/function in objective function of (5) is in a form of $y \log(1 + \frac{x}{y})$ which is jointly concave with respect to x and y .

consider the first-order derivative of (6) in terms of θ_k and set it to zero, as follows:

$$\log \left(1 + \frac{t_k P_B \text{Tr}(\mathbf{g}_k \mathbf{g}_k^H \mathbf{Q})}{\theta_k} \right) - \frac{t_k P_B \text{Tr}(\mathbf{g}_k \mathbf{g}_k^H \mathbf{Q})}{\theta_k + t_k P_B \text{Tr}(\mathbf{g}_k \mathbf{g}_k^H \mathbf{Q})} = \nu. \quad (9)$$

From (9), it is easily verified that $f(y) = \log(1 + y) - \frac{y}{1+y}$ is a monotonically increasing function with respect to y . Thus, in order to satisfy the above K equations in (9), we have the following equations:

$$\frac{t_1 P_B \text{Tr}(\mathbf{g}_1 \mathbf{g}_1^H \mathbf{Q})}{\theta_1} = \dots = \frac{t_K P_B \text{Tr}(\mathbf{g}_K \mathbf{g}_K^H \mathbf{Q})}{\theta_K}. \quad (10)$$

Let $\frac{1}{\rho} = \frac{t_k P_B \text{Tr}(\mathbf{g}_k \mathbf{g}_k^H \mathbf{Q})}{\theta_k}$, we have

$$\theta_k = \rho t_k P_B \text{Tr}(\mathbf{g}_k \mathbf{g}_k^H \mathbf{Q}). \quad (11)$$

Substitute the above equality into the constraint (5a),

$$\rho \sum_{k=1}^K t_k P_B \text{Tr}(\mathbf{g}_k \mathbf{g}_k^H \mathbf{Q}) = 1 - \theta_0, \Rightarrow \rho = \frac{1 - \theta_0}{\sum_{k=1}^K t_k P_B \text{Tr}(\mathbf{g}_k \mathbf{g}_k^H \mathbf{Q})}. \quad (12)$$

From (11) and (12), the optimal solution to θ_k is derived as a function with respect to θ_0 for a given \mathbf{Q} , as follows:

$$\theta_k^* = \frac{(1 - \theta_0) t_k \text{Tr}(\mathbf{g}_k \mathbf{g}_k^H \mathbf{Q})}{\sum_{k=1}^K t_k \text{Tr}(\mathbf{g}_k \mathbf{g}_k^H \mathbf{Q})}. \quad (13)$$

Substitute (13) into (5), we have the following problem

$$\max_{\theta_0 \in (0,1), \mathbf{Q} \succeq \mathbf{0}} (1 - \theta_0) \log \left(1 + \frac{P_B \sum_{k=1}^K t_k \text{Tr}(\mathbf{g}_k \mathbf{g}_k^H \mathbf{Q})}{1 - \theta_0} \right) \text{ s.t. } \text{Tr}(\mathbf{Q}) \leq \theta_0. \quad (14)$$

The problem (14) can be equivalently written as

$$\max_{\theta_0 \in (0,1), \mathbf{Q} \succeq \mathbf{0}} (1 - \theta_0) \log \left(1 + \frac{P_B \text{Tr}(\mathbf{G} \mathbf{G}^H \mathbf{Q})}{1 - \theta_0} \right) \text{ s.t. } \text{Tr}(\mathbf{Q}) \leq \theta_0, \quad (15)$$

where $\mathbf{G} = [\sqrt{t_1} \mathbf{g}_1, \dots, \sqrt{t_K} \mathbf{g}_K]$. In order to solve (15), we temporarily fix θ_0 and find the optimal solution \mathbf{Q}^* by solving the following optimization problem:

$$\max_{\mathbf{Q} \succeq \mathbf{0}} \text{Tr}(\mathbf{G}^H \mathbf{Q} \mathbf{G}), \text{ s.t. } \text{Tr}(\mathbf{Q}) \leq \theta_0. \quad (16)$$

To that end, we introduce the following lemma.

Lemma 2: The optimal solution to (16) is given by $\mathbf{Q}^* = \theta_0 \mathbf{v}_{\max}(\mathbf{G} \mathbf{G}^H) \mathbf{v}_{\max}(\mathbf{G} \mathbf{G}^H)^H$.

Proof: Please refer to [4]. ■

Given \mathbf{Q}^* and exploiting Lemma 2, (15) can be rewritten with respect to θ_0 as follows:

$$\max_{\theta_0 \in (0,1)} (1 - \theta_0) \log \left(1 + \frac{\theta_0}{1 - \theta_0} P_B \lambda_{\max}(\mathbf{G} \mathbf{G}^H) \right). \quad (17)$$

Although the optimal energy time allocation θ_0^* can be attained by using one-dimensional line search, e.g., golden search, we propose a closed-form solution to achieve θ_0^* without using such an exhaustive search.

Lemma 3: The optimal energy time allocation θ_0^* can be

obtained by

$$\theta_0^* = \frac{e^{\mathcal{W}(\frac{P_B \lambda_{\max}(\mathbf{G}\mathbf{G}^H)-1}{e})+1} - 1}{P_B \lambda_{\max}(\mathbf{G}\mathbf{G}^H) - 1 + e^{\mathcal{W}(\frac{P_B \lambda_{\max}(\mathbf{G}\mathbf{G}^H)-1}{e})+1}}, \quad (18)$$

where $\mathcal{W}(x)$ is the Lambert W function.

Proof: See Appendix B. ■

The proposed closed-form solution to problem (5) is summarized in **Algorithm 1**.

Algorithm 1 Closed-form solution

- 1: Input: \mathbf{G} , P_B
 - 2: $\mathbf{w}^* = \mathbf{v}_{\max}(\mathbf{G}\mathbf{G}^H)$
 - 3: Obtain θ_0^* using (18)
 - 4: $\mathbf{Q}^* = \theta_0^* \mathbf{w}^* \mathbf{w}^{*H}$
 - 5: Obtain $\theta_k^* = \frac{(1-\theta_0^*)t_k \text{Tr}(\mathbf{g}_k \mathbf{g}_k^H \mathbf{Q}^*)}{\sum_{n=1}^K t_n \text{Tr}(\mathbf{g}_n \mathbf{g}_n^H \mathbf{Q}^*)} \forall k \in \{1, \dots, K\}$
 - 6: Output: \mathbf{w}^* , θ_0^* , and θ_k^* , $\forall k \in \{1, \dots, K\}$
-

IV. ENERGY TRADING OR SOCIAL WELFARE BASED SUM THROUGHPUT OPTIMIZATION

In this section, we consider a more practical scenario that the PS and the sensor network belong to different service operators. Specifically, monetary payments are required by the sensor network to purchase the energy services released from the PS to support WIT. In the following, we first introduce a *quadratic energy trading* process, which formulates this case as a *Stackelberg* game. Then *linear energy trading* based *Stackelberg* game is studied to provide a comparison. In addition, we formulate a *social welfare* scheme to capture the ‘‘cooperative’’ energy interaction between the PS and the sensor network. For the formulated *Stackelberg* games, we analyze the associated *Stackelberg* equilibrium, where both the WET network and the sensor network reach an agreement on power allocation and energy price to achieve the maximum sum throughput of the sensor network. While, the *social welfare* scheme aims to obtain the optimal power allocation to maximize the sum throughput.

A. Quadratic Energy Trading based Stackelberg Game

In this scheme, there is no cooperation between the PS and the sensor network. Instead, the sensor network purchases energy services from the PS. *quadratic energy trading* is introduced to exploit the strategic behaviors of these two networks and then the energy interaction is formulated as a *Stackelberg* game.

1) Stackelberg Game Formulation:

- **Leader:** The sensor network plays the leader role and announces/pays a price for the energy services provided by the PS. The leader maximizes its utility function defined as the difference between the benefits obtained from the achievable sum throughput and the payment for the energy services. Thus, the *leader-level* problem can

be formulated as:

$$\begin{aligned} \max_{\theta_0, \tau} U_L(P_B, \tau, \theta_0) &= \mu(1 - \theta_0) \log \left(1 + \frac{\theta_0 P_B \lambda_{\max}(\mathbf{G}\mathbf{G}^H)}{1 - \theta_0} \right) \\ &\quad - \tau \theta_0 P_B, \\ \text{s.t. } 0 &< \theta_0 < 1, \end{aligned} \quad (19)$$

where $\mu > 0$ is the price per unit sum throughput of the sensor network; τ denotes the energy price paid by the sensor network.

- **Follower:** The PS is the follower and optimizes its transmit power based on the energy price announced by the leader. Specially, the follower maximizes its own utility function defined as the difference between the energy payment and its quadratic operation cost.

$$\max_{P_B} U_E(P_B, \tau, \theta_0) = \tau \theta_0 P_B - \theta_0 \mathcal{F}(P_B), \quad \text{s.t. } P_B \geq 0, \quad (20)$$

where $\mathcal{F}(x) = Ax^2 + Bx$ (A and B are pre-determined parameters) is a quadratic function⁵, which is employed to model the cost of the PS per unit time for wirelessly charging the sensor nodes with the transmit power P_B .

In the sequel, we analyze the optimal strategies for both PS and sensor network to derive the *Stackelberg* equilibrium of the formulated game in order to maximize their own utility functions.

2) *Stackelberg Equilibrium:* In this subsection, we derive the *Stackelberg* equilibrium for the formulated game in Section IV-A1, which can be formally defined as:

Definition 1: Let (θ_0^*, τ^*) denote the solutions to the problem (19), while P_{BS}^* represents the solution to the problem (20). The tuple $(P_B^*, \theta^*, \lambda^*)$ is the *Stackelberg* equilibrium of the formulated game provided that the following conditions are satisfied.

$$U_L(P_B^*, \tau^*, \theta_0^*) \geq U_L(P_B^*, \tau, \theta_0), \quad (21)$$

$$U_E(P_B^*, \tau^*, \theta_0^*) \geq U_E(P_B, \tau^*, \theta_0^*), \quad (22)$$

for $0 < \theta_0 < 1$, $\tau \geq 0$, and $P_B \geq 0$.

According to *Definition 1*, we first derive the closed-form optimal power allocation P_B by solving the follower game (20). Given θ_0^* and τ^* announced by the leader game (19), (20) is a convex optimization problem since its objective function is a quadratic function in terms of P_B with a linear constraint. Hence, the optimal solution P_B^* can be given in the following *lemma*:

Lemma 4: The optimal solution to the problem (20) is

$$P_B^* = \left[\frac{\tau - B}{2A} \right]^+. \quad (23)$$

Proof: The proof of this *lemma* can be derived by taking into consideration that the first derivatives to the objective function in (20) equals to zero. However, it is omitted here due to space limitation. ■

With a given optimal transmit power P_B^* of the PS, the

⁵Note that this quadratic function has been applied in the energy market to model the energy cost [25].

leader problem (19) can be rewritten as

$$\max_{\theta_0 \in (0,1), \tau \geq 0} U_L(\tau, \theta_0) = \mu(1-\theta_0) \log \left(1 + \frac{\theta_0 \lambda_{\max}(\mathbf{G}\mathbf{G}^H) (\tau - B)}{1-\theta_0} \frac{(\tau - B)}{2A} \right) - \tau \theta_0 \frac{(\tau - B)}{2A}. \quad (24)$$

From (24), it is hard to find the optimal solutions of τ and θ_0 at the same time due to the complexity of its objective function. In order to circumvent this issue, we propose a two-step approach to solve (24). We first derive the optimal closed-form solution to τ for a given θ_0 . Then, the optimal value for θ_0 can be achieved via a numerical search.

First, we derive the optimal solution for τ by introducing the following lemma.

Lemma 5: The optimal solution τ^* can be derived as

$$\tau^* = \frac{-\theta_0(1-3bD) + \sqrt{\theta_0^2(1-bD)^2 + 2\theta_0 ab^2 C}}{2\theta_0 bC}, \quad (25)$$

where $a = \mu(1-\theta_0)$, $b = \frac{\theta_0 \lambda_{\max}(\mathbf{G}\mathbf{G}^H)}{1-\theta_0}$, $C = \frac{1}{2A}$, $D = \frac{B}{4A}$.

Proof: See Appendix C. ■

Next, substituting τ^* into (24), we have the following optimization problem with respect to θ_0 :

$$\max_{\theta_0 \in (0,1)} U_L(\theta_0, \tau^*) = \mu(1-\theta_0) \log \left(1 + \frac{\theta_0}{1-\theta_0} d_1 \right) - \theta_0 d_2, \quad (26)$$

where $d_1 = P_B^* \lambda_{\max}(\mathbf{G}\mathbf{G}^H)$ and $d_2 = \tau P_B^*$. It is easily verified that (26) is a convex optimization problem, however, it is hard to find the closed-form optimal solution for θ_0 . Thus, the optimal solution for θ_0 can be efficiently achieved via numerical search, which can be given by

$$\theta_0^* = \arg \max_{\theta_0 \in (0,1)} U_L(\theta_0, \tau^*). \quad (27)$$

The *Stackelberg equilibrium* for the formulated game, i.e., P_B^* , τ^* , and θ_0^* , can be obtained via (23), (25) and (27).

B. Linear Energy Trading based Stackelberg Game

In the previous subsection, we exploit the *quadratic energy trading* between the PS and the sensor nodes, where the *quadratic energy trading based Stackelberg* is proposed. As a comparison, in this subsection, we propose *linear energy trading based Stackelberg* game to exploit the energy interaction between the PS and the sensor nodes with a fixed energy transfer time allocation θ_0 . In this formulated game, the PS is modeled as the leader determining the energy price to maximize its own utility, which is defined as the difference between the payment from the WSNs and the linear energy transfer cost. Thus, the utility function of the hybrid BS can be written as

$$U_E = (\tau - \kappa)\theta P_B, \quad (28)$$

where τ denotes the energy price released from the PS, κ captures the operational cost per unit transmit power. Note that κ satisfies $\kappa \leq \tau$ to guarantee the utility function (28) is non-negative, whereas if $\kappa \geq \tau$, which means that the PS would refuse to sell the energy.

Remark 1: From (28), one can observe that the PS's utility function is a linear function with respect to κ , which is the

linear energy operation cost per unit transmit power. However, (28) is a concave function in terms of τ , which is shown in the following.

Stackelberg Game Leader Level

$$\max_{\tau} U_E, \text{ s.t. } \tau \geq \kappa \geq 0. \quad (29)$$

In addition, the sensor nodes play the follower's role to guarantee that they can harvest sufficient energy to transmit the monitoring data to the FC. Specifically, these nodes aim to maximize their own utility function defined as the gap between the benefits of the achievable sum throughput and their total payments to the PS for wireless energy transfer.

Stackelberg Game Follower Level

$$\max_{\theta, P_{BS}} U_L(\theta, P_B), \text{ s.t. } 0 \leq \theta \leq 1, P_B \geq 0. \quad (30)$$

where

$$U_L(\theta, P_B) = \mu(1-\theta) \log \left(1 + \frac{\theta P_B \lambda_{\max}(\mathbf{G}\mathbf{G}^H)}{1-\theta} \right) - \tau \theta P_B.$$

Then, we focus on the optimal solution of the PS's transmit power by solving the problem (30). It is easily verified that the utility function in (31) is a concave function with respect to P_{BS} . Now, we set its first-order derivative equal to zero,

$$\frac{\partial U_L}{\partial P_{BS}} = \frac{\mu \theta_0 \lambda_{\max}(\mathbf{G}\mathbf{G}^H)}{1 + \frac{\theta_0 P_B \lambda_{\max}(\mathbf{G}\mathbf{G}^H)}{1-\theta_0}} - \tau \theta_0 = 0. \quad (31)$$

After some mathematical manipulations, the optimal power allocation of the PS with respect to λ is given by

$$P_B^*(\lambda) = \left[\frac{\mu(1-\theta_0)}{\theta_0 \tau} - \frac{1-\theta_0}{\theta_0 \lambda_{\max}(\mathbf{G}\mathbf{G}^H)} \right]^+. \quad (32)$$

Substituting (32) into (29) yields

$$U_{BS} = (\tau - \kappa)\theta_0 P_B^*(\lambda). \quad (33)$$

Taking the first-order derivative to (33) and setting it to zero, we obtain

$$\begin{aligned} \frac{\partial U_E}{\partial \tau} &= \theta_0 \left(\frac{\mu(1-\theta_0)}{\theta_0 \tau} - \frac{1-\theta_0}{\theta_0 \lambda_{\max}(\mathbf{G}\mathbf{G}^H)} \right) \\ &\quad + (\tau - \kappa)\theta_0 \left(-\frac{\mu(1-\theta_0)}{\tau^2 \theta_0} \right) = 0, \\ \Rightarrow \frac{1-\theta_0}{\lambda_{\max}(\mathbf{G}\mathbf{G}^H)} &= \frac{\kappa \mu(1-\theta_0)}{\tau^2} \end{aligned} \quad (34)$$

By solving the equation (34), the optimal energy transfer price τ^* is given by

$$\tau^* = [\kappa \mu \lambda_{\max}(\mathbf{G}\mathbf{G}^H)]^{\frac{1}{2}}. \quad (35)$$

Thus, the optimal power allocation of the PS can be achieved by substituting (35) into (32) as

$$P_B^* = \left[\frac{\mu(1-\theta_0)}{\theta_0 \sqrt{\kappa \mu \lambda_{\max}(\mathbf{G}\mathbf{G}^H)}} - \frac{1-\theta_0}{\theta_0 \lambda_{\max}(\mathbf{G}\mathbf{G}^H)} \right]^+. \quad (36)$$

Note that both U_E and U_L are concave functions in terms of τ and P_B for a fixed θ_0 . Thus, we have completed the derivations of the Stackelberg equilibrium (τ^* , P_B^*) for the formulated Stackelberg game shown in (36) and (35).

C. Social Welfare Scheme

In Section IV-A and Section IV-B, *quadratic energy trading* and *linear energy trading* based *Stackelberg* games are formulated to exploit the hierarchical energy interaction between the PS and the sensor network. However, these two game based schemes may lead to the performance loss of both PS and the sensor network due to the possible selfish behaviors of these players. In order to circumvent this issue, we propose in the following a *social welfare* scheme, where cooperation between the WET and sensor network is allowed. This scheme does not consider the energy price. Instead, the PS and the sensor network cooperatively maximize a *social welfare*, which is defined as the difference between the benefits obtained from the sum throughput at the sensor network and the *quadratic* energy transfer operation cost of the PS. This *social welfare* maximization is performed by jointly optimizing the energy transfer time allocation and the transmit power of the PS. Mathematically, the *social welfare* utility function can be formulated as

$$U_{SW}(P_B, \theta_0) = \mu(1-\theta_0) \log \left(1 + \frac{\theta_0 \lambda_{\max}(\mathbf{G}\mathbf{G}^H)}{1-\theta_0} P_B \right) - \theta_0 (AP_B^2 + BP_B). \quad (37)$$

Thus, the *social welfare* maximization problem is given by

$$\max_{P_B, \theta_0} U_{SW}(P_B, \theta_0), \quad s.t. \quad P_B \geq 0, \quad 0 < \theta_0 < 1. \quad (38)$$

It is easily verified that (38) is a convex optimization problem due to the concave function (37) and the linear constraints. Hence, we first take the first-order derivative of (37) with respect to P_B for a given θ_0 , and set it to zero.

$$\frac{\partial U_{SW}}{\partial P_B} = \frac{ab}{1 + P_B b} - (2A\theta_0 P_B + B\theta_0) = 0, \quad (39)$$

where a and b have been defined in (25). After some mathematical manipulations, we have

$$P_B^* = \frac{-(2A\theta_0 + Bb\theta_0) + \sqrt{(2A\theta_0 - Bb\theta_0)^2 + 8Aab^2\theta_0}}{4Ab\theta_0}. \quad (40)$$

Then, we substitute the optimal solution P_B^* (40) into (38), the optimal energy time allocation θ_0^* can be achieved via numerical search similar to (27).

V. NUMERICAL RESULTS

In this section, simulation results are provided to validate our theoretical derivations in Section III and IV. In simulation, we consider a wireless powered sensor network that consists of one PS equipped with four transmit antennas, i.e., $N_T = 4$, four single-antenna sensor nodes, i.e., $K = 4$, and a single-antenna FC. It is assumed that the channel coefficient g_k between the PS and \mathcal{U}_k is modeled as $|g_k|^2 = A(d_{DL}^k)^{-\alpha} \mathbf{g}$, where $A = 10^{-3}$, $\alpha = 3$ is the path loss exponent, d_{DL}^k denotes the distance between the PS and \mathcal{U}_k , and $\mathbf{g} \sim \mathcal{CN}(0, \mathbf{I})$. Similarly the channel coefficient between \mathcal{U}_k and the FC, i.e., h_k , is modeled as $|h_k|^2 = A(d_{UL}^k)^{-\alpha} h$, where h follows the standard Rayleigh fading and d_{UL}^k is the distance between \mathcal{U}_k and the FC. Without loss of generality, we assume $d_{DL}^k = d_{DL}$, $d_{UL}^k = d_{UL}$, and the total distance between the PS and the FC is set to be $d = d_{DL} + d_{UL}$. The maximum transmit power P_B is set to be 1 W, i.e., 30 dBm,

unless otherwise stated. The noise power is assumed to be $\sigma^2 = 10^{-8}$ W, and the energy harvesting efficiency is assumed to be $\xi_k = \xi = 0.5$ at $\mathcal{U}_k, \forall k$.

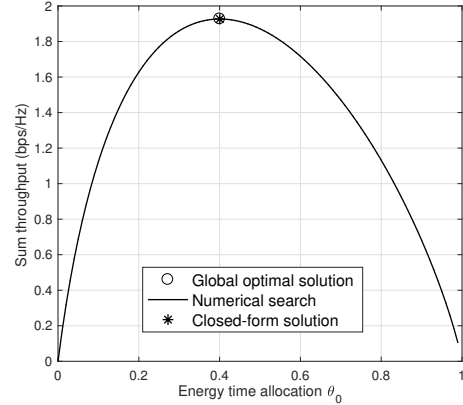


Fig. 2: Sum throughput versus energy time allocation θ_0 .

A. Sum Throughput Optimization

First, we evaluate the performance of the joint-optimization approach, where both PS and sensor network belong to the same service operator. Fig. 2 shows the sum throughput, obtained by exhaustive/numerical search, versus the energy time allocation θ_0 . From this result, one can observe that the sum throughput function is a concave function. As comparison, both global optimal solution and closed-form solution are presented. Optimization package CVX [26] is utilized to solve problem (5) while Algorithm 1 is executed to obtain the closed-form solution. It is clear that both solutions yield identical results which validates the accuracy of the proposed closed-form solution.

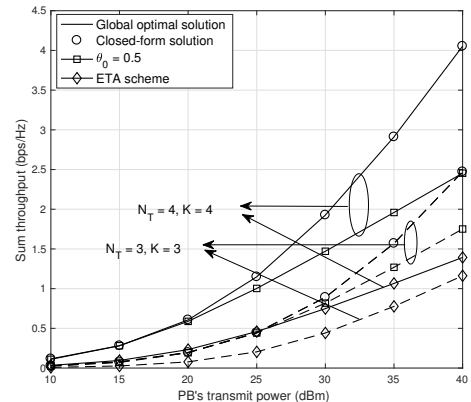


Fig. 3: Sum throughput versus PS's transmit power P_B .

In Fig. 3, the sum throughputs obtained by our proposed approaches, the fixed energy time allocation scheme (i.e., $\theta_0 = 0.5$) as well as the equal time allocation (ETA) scheme in [12] are shown versus the PS's transmit power P_B . It is clear that the sum throughput increases as either P_B or N_T or K

increases. The results again confirm that the proposed closed-form solution attains the same performance as the proposed global optimal solution does. It can be observed that both of our proposed solutions outperform the scheme with $\theta_0 = 0.5$ and the ETA scheme.

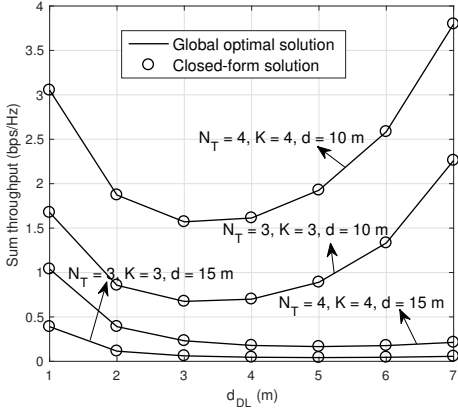


Fig. 4: Sum throughput versus d_{DL} .

Then, we evaluate the impact of the sensor deployment to the sum throughput. In Fig. 4, the sum throughput is plotted versus the distance between the PS and a sensor, i.e., d_{DL} with different total distances between the PS and the FC, i.e., $d = 10$ m and 15 m. It can be seen from the figure that at a given d_{DL} , the sum throughput decreases as d increases. This is due to a fact that the channel path loss between the sensors and the FC increases. When the distance between the PS and the FC is 10 m, deploying sensors closer to the FC results in a higher sum throughput. However, when the distance between the PS and the FC is 15 m, sensors should be placed nearer to the PS in order to obtain a higher throughput.

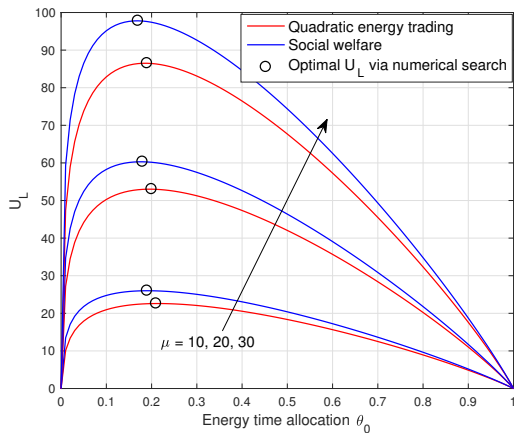


Fig. 5: U_L versus energy time allocation θ_0 .

B. Energy Interaction Approaches

Next, we evaluate the performance of the energy-interaction approach, where both PS and sensor network belong to different service operators. In Fig. 5, the utility functions of

the sensor network for both *quadratic energy trading* based *Stackelberg* game and *Social welfare* scheme are plotted versus the energy time allocation θ_0 . From the figure, one can easily observe that utility functions are concave functions in terms of θ_0 . To compare, a numerical/exhaustive search is performed for the utility function of the sensor network and the results are shown in the figure. It is clear that the numerical/exhaustive search obtains the optimal energy time allocation, i.e., θ_0^* . It can also be observed that the *Social welfare* scheme outperforms the *quadratic energy trading* based *Stackelberg* game in terms of utility function. This is due to the fact that the PS is selfless in the *Social welfare* scheme but not in the *quadratic energy trading* based *Stackelberg* game.

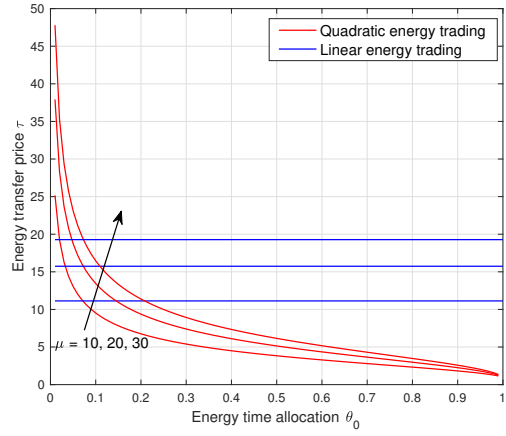


Fig. 6: Energy price versus energy time allocation θ_0 .

In Fig. 6, we plot the energy price τ versus the energy time allocation θ_0 for the *quadratic* and *linear energy trading* based *Stackelberg* games. From this result, it is easily observed that the *quadratic energy trading* scheme decreases as θ_0 in terms of the energy price paid by the WSN. This is owing to a fact that a larger θ_0 leads to the lower prices to be paid by the WSN. Whereas the energy transfer price is a constant in the *linear energy trading*, which confirms that (35). In addition, the WSN pays a higher price when employing *quadratic energy trading* scheme than employing *linear energy trading* in low energy time allocation regimes. However, the *quadratic energy trading* shows its financial advantage over the *linear energy trading* after $\theta_0 \approx 0.1$, since the former pays lower energy price than the latter.

Fig. 7 evaluates the power consumption of the PS versus the energy time allocation θ_0 in the three proposed schemes. From this result, one can observe that the three schemes decrease with θ_0 in terms of power consumption. This is owing to a fact that a larger θ_0 allocated for WET phase will lead to a smaller power consumption. In addition, it is interesting that both *quadratic energy trading* based *Stackelberg* game and *social welfare* scheme consume less power than the *linear energy trading* based *Stackelberg* game in the low energy time regime. However, this trend will be reversed as θ_0 increases in the high energy time regime.

Then, we evaluate the utility function of these three schemes. Fig. 8 shows that the utility function versus the

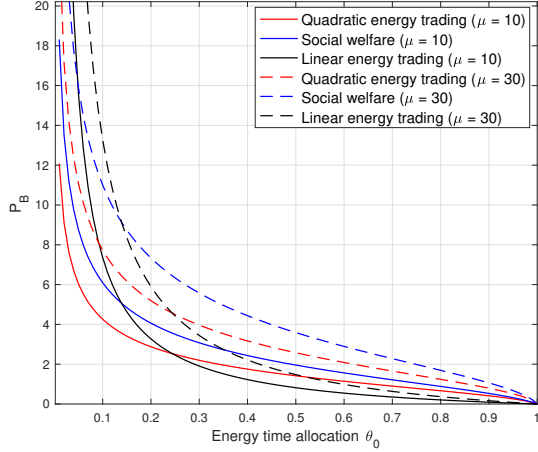


Fig. 7: P_B versus energy time allocation θ_0 .

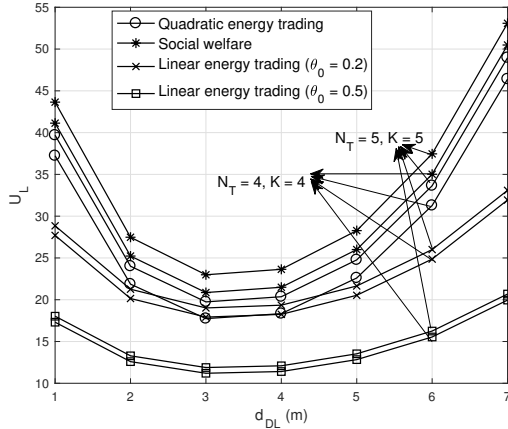


Fig. 8: U_L versus d_{DL} .

distance between the PS and the sensor nodes d_{DL} . From this result, the utility functions of the sensor network for the quadratic energy trading based *Stackelberg* game, the *Social welfare* scheme and the linear energy trading based *Stackelberg* game are plotted versus the distance between the PS and the sensors, i.e., d_{DL} , with total distance between the PS and the FC, i.e., $d = 10$ m. It can be seen from the figure that at a given d_{DL} , the utility function decreases first and then increases after $d_{DL} \approx 3$ m. This means that we deploy the sensors closer to the FC results to achieve a higher utility. It also can be observed that both *quadratic energy trading* based *Stackelberg* game and *social welfare* scheme outperforms the *linear energy trading* based *Stackelberg* game, which highlight our proposed *quadratic energy trading interaction* between the WET and the sensor network.

In Fig. 9, we evaluate the utility function versus the EH efficiency ξ , where the utility of these three schemes increases as ξ increases. While Fig. 10 shows that the utility function with different number of sensors K , where it confirms that a larger number of sensor nodes K will lead to the increasing of utility for these three schemes. From Fig. 9 and Fig. 10, we also observe that both *quadratic energy trading* based

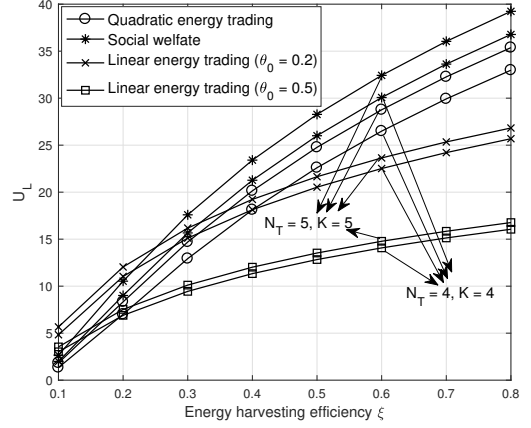


Fig. 9: U_L versus ξ .

game and *social welfare* scheme perform better than the *linear energy trading* based game. This is because, the *quadratic energy trading* process outperforms the *linear energy trading* process, which confirms the advantage of our proposed *quadratic energy trading interaction*.

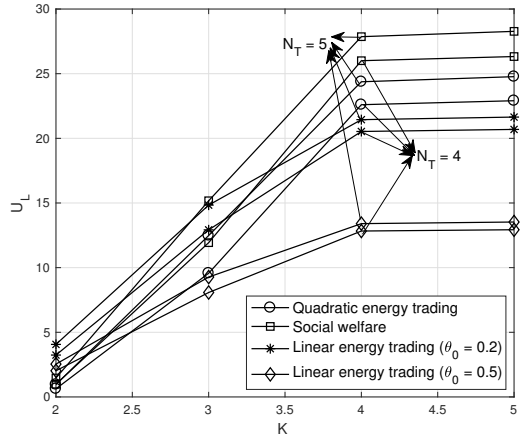


Fig. 10: U_L versus K .

Finally, we compare the proposed cooperative sum throughput scheme⁶ and the proposed energy interaction schemes.⁷ Fig. 11 shows that the sum throughput performance versus the distance between the PS and the sensor nodes d_{DL} . It can be observed that the cooperative sum throughput scheme outperforms these three energy interaction schemes in terms of the sum throughput. This is owing to a fact that there is a cooperation between both WET and sensor networks such that the cooperative sum throughput scheme does not need to make payment for the energy transfer. Meanwhile, both WET and sensor networks operate in a competitive manner in the

⁶The cooperative sum throughput scheme exploits the STM problem, where the global and closed-form optimal solutions are achieved via CVX package and **Algorithm 1**, respectively.

⁷The energy interaction schemes include *quadratic energy trading* based *Stackelberg* game, *linear energy trading* based *Stackelberg* game, and *social welfare* scheme.

proposed energy interaction schemes, in which the incentives are required by the PS for the energy service to assist the WIT in the sensor network, leading to the *energy trading* payment. This comparison confirms the advantage of the cooperative sum throughput scheme. In addition, the fixed time allocation scheme (i.e., $\theta_0 = 0.5$) outperforms the *linear energy trading* based *Stackelberg* game in terms of the sum throughput. Fig. 12 shows that the sum throughput performance versus the number of sensor nodes (i.e., K). From this result, one can observe that the cooperative sum throughput scheme outperforms the energy interaction schemes when $K \leq 7$. After that the cooperative sum throughput scheme still increases slowly but it falls below the sum throughput in the energy interaction schemes. However, the sum throughput in the *quadratic energy trading* based *Stackelberg* game decreases after $K = 8$ and becomes lower than the cooperative scheme again when $K = 10$. Additionally, the fixed time allocation scheme (i.e., $\theta_0 = 0.5$) outperforms the *linear energy trading* based *Stackelberg* game, which highlights the advantage of the cooperative sum throughput scheme.

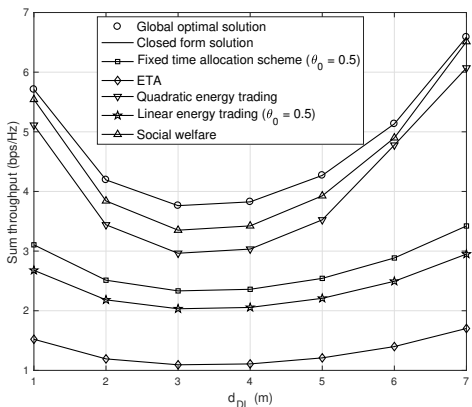


Fig. 11: Sum throughput versus energy time allocation d_{DL} .

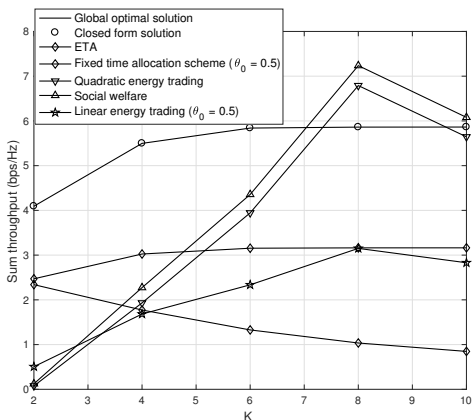


Fig. 12: Sum throughput versus K .

VI. CONCLUSION

This paper investigated a WPSN in IoT system, where a PS provides power wirelessly to multiple sensor nodes which

send their monitor data to the FC. We first considered an ideal scenario where the PS and sensor network belong to the same service provider. In this case, we maximized the system sum throughput to jointly optimize the energy beamforming vector and time allocation. Then, for the second scenario where the PS and the sensor network belong to the different providers, we formulated *quadratic energy trading* and *linear energy trading* based *Stackelberg* games as well as the *social welfare* scheme. A higher utility level is achieved if social welfare responsibility is taken into account as all parties work together to maximize a common target. At the same time, the energy buyer, i.e., the sensor network, would have to pay a higher price for energy purchase if the seller, i.e., the PS, has a monopoly authority to dictate and lead the market, as shown in the non-energy trading scenario. However, in an environment where there are potential competitors for energy selling, the sensor customer can become the leader who would negotiate for a much better energy price, as reflected in the energy trading case of our proposed game. Numerical results were provided to validate our proposed schemes and showed that both energy trading and social welfare schemes provide a better energy cost efficiency. For future works, we can consider a more challenging scenario such that each sensor node works in the full-duplex (FD) mode. Specifically, the FD operation of the sensor nodes enables the simultaneous transmission/reception of information signals/energy in the downlink and uplink, respectively. In addition, the sensor nodes can employ the harvested energy to transmit a series of information data to the FC during multiple time periods, which leads to the energy and data queues at each sensor node. These would change the dynamic of the optimization problems, which may require different design/solutions.

APPENDIX A PROOF OF LEMMA 1

Provided that the optimal energy time allocation to (5) exists, and for given θ , we consider the following problem

$$\begin{aligned} \max_{\mathbf{Q}} \quad & \sum_{k=1}^K \theta_k \log \left(1 + \frac{t_k P_B \text{Tr}(\mathbf{g}_k \mathbf{g}_k^H \mathbf{Q})}{\theta_k} \right), \\ \text{s.t.} \quad & \text{Tr}(\mathbf{Q}) \leq \theta_0, \quad \mathbf{Q} \succeq \mathbf{0}. \end{aligned} \quad (41)$$

The objective function in (41) is concave but nonlinear. In order to linearize this objective function, we consider the successive convex approximation (SCA) to convert (41) into a series of linear programming (LP) as follows.

$$\begin{aligned} \mathbf{Q}^{(n+1)} = \arg \max_{\mathbf{Q}} \quad & \sum_{k=1}^K \frac{t_k P_B \text{Tr}(\mathbf{g}_k \mathbf{g}_k^H \mathbf{Q})}{1 + \frac{t_k P_B \text{Tr}(\mathbf{g}_k \mathbf{g}_k^H \mathbf{Q}^{(n)})}{\theta_k}} \\ \text{s.t.} \quad & \text{Tr}(\mathbf{Q}) \leq \theta_0, \quad \mathbf{Q} \succeq \mathbf{0}, \end{aligned} \quad (42)$$

where $\mathbf{Q}^{(n)}$ is the optimal solution at n -th iteration. According to [27], it is clear that $\mathbf{Q}^{(n+1)}$ can be achieved by solving (42) and yields a rank-one solution.

Sine \mathbf{Q}^* is a rank-one matrix and $\mathbf{Q} = \theta_0 \mathbf{W}$, \mathbf{W}^* is also a rank-one matrix.

APPENDIX B
PROOF OF LEMMA 3

Define $c = P_B \lambda_{\max}(\mathbf{G}\mathbf{G}^H)$, we write the sum throughout

$$T(\theta_0) = (1 - \theta_0) \log \left(1 + \frac{\theta_0}{1 - \theta_0} c \right). \quad (43)$$

We take the first-order derivatives of $T(\theta_0)$ with respect to θ_0 , and set $\frac{\partial T(\theta_0)}{\partial \theta_0} = 0$,

$$c + \frac{\theta_0}{1 - \theta_0} c = \left(1 + \frac{\theta_0}{1 - \theta_0} c \right) \ln \left(1 + \frac{\theta_0}{1 - \theta_0} c \right). \quad (44)$$

Let $z = 1 + \frac{\theta_0}{1 - \theta_0} c$, the above equality can be modified as

$$c - 1 + z = z \ln z. \quad (45)$$

After a series of mathematical manipulations, we have

$$\ln \left(\frac{z}{e} \right) e^{\ln \left(\frac{z}{e} \right)} = \frac{c - 1}{e}. \quad (46)$$

The equation (46) is a standard Lambert W function. Hence, we have

$$\ln \left(\frac{z}{e} \right) = \mathcal{W} \left(\frac{c - 1}{e} \right). \quad (47)$$

After some mathematical manipulations, the optimal energy time allocation θ_0^* can be given by

$$\theta_0^* = \frac{e^{\mathcal{W} \left(\frac{c-1}{e} \right) + 1} - 1}{c - 1 + e^{\mathcal{W} \left(\frac{c-1}{e} \right) + 1}}. \quad (48)$$

We have completed *Lemma 3*.

APPENDIX C
PROOF OF LEMMA 5

It is easily verified that the objective function in (24) is a concave function in terms of τ for a given θ . Thus, in order to find the optimal solution to τ , we consider its first-order derivatives that equals to zero as

$$\frac{\partial U_L}{\partial \tau} = \frac{abC}{1 + b(\tau C - D) - bD} - 2\theta_0(\tau C - D) = 0. \quad (49)$$

After a few of mathematical manipulations, we have

$$2\theta_0 b(\tau C - D)^2 + 2\theta_0(1 - bD)(\tau C - D) - abC = 0. \quad (50)$$

By solving the above equation, we can obtain

$$\begin{cases} \tau_1 = \frac{-\theta_0(1-3bD) + \sqrt{\theta_0^2(1-bD)^2 + 2\theta_0 ab^2 C}}{2\theta_0 b C}, \\ \tau_2 = \frac{-\theta_0(1-3bD) - \sqrt{\theta_0^2(1-bD)^2 + 2\theta_0 ab^2 C}}{2\theta_0 b C} \end{cases}, \quad (51)$$

Now, let us verify the validity of both solutions shown in (51). The objective function (24) includes the logarithm term, which should be non-negative. Thus, we check the validity of these solutions by substituting τ_1 and τ_2 into the logarithm term of (24), respectively. We first check τ_1 as follows:

$$\begin{aligned} & 1 + b \left(\frac{-\theta_0(1-3bD) + \sqrt{\theta_0^2(1-bD)^2 + 2\theta_0 ab^2 C}}{2\theta_0 b} - 2D \right) \\ & > 1 + b \left(\frac{-\theta_0(1-bD) + \theta_0|1-bD|}{2\theta_0 b} \right) \geq 1. \end{aligned} \quad (52)$$

Similarly, we check τ_2 as

$$1 + b \left(\frac{-\theta_0(1-3bD) - \sqrt{\theta_0^2(1-bD)^2 + 2\theta_0 ab^2 C}}{2\theta_0 b} - 2D \right) < 1 \quad (53)$$

Thus, τ_1 is a valid stationary point. Due to the concavity of the objective function in (24), its second-order derivatives with respect to τ is less than zero, which indicates that its maximum value is the stationary point τ_1 . Also, it is easily verified that $\tau_1 > 0$, which satisfies the constraint in (24). Thus, the optimal solution to the problem (24), denoted by τ^* , is the stationary point τ_1 , which completes the proof.

REFERENCES

- [1] E. Ahmed, I. Yaqoob, A. Gani, M. Imran, and M. Guizani, "Internet-of-things-based smart environments: state of the art, taxonomy, and open research challenges," *IEEE Wireless Commun.*, vol. 23, no. 5, pp. 10–16, Oct. 2016.
- [2] J. Yick, B. Mukherjee, and D. Ghosal, "Wireless sensor network survey," *Comput. Networks*, vol. 52, no. 12, pp. 2292–2330, Aug. 2008.
- [3] I. Akyildiz, W. Su, Y. Sankarasubramaniam, and E. Cayirci, "Wireless sensor networks: a survey," *Computer Networks*, vol. 38, no. 4, pp. 393–422, 2002.
- [4] R. Zhang and C. K. Ho, "MIMO broadcasting for simultaneous wireless information and power transfer," *IEEE Trans. Wireless Commun.*, vol. 12, pp. 1989–2001, May 2013.
- [5] S. Sudevalayam and P. Kulkarni, "Energy harvesting sensor nodes: Survey and implications," *IEEE Commun. Surveys Tut.*, vol. 13, pp. 443–461, Third 2011.
- [6] O. Ozel, K. Tutuncuoglu, J. Yang, S. Ulukus, and A. Yener, "Transmission with energy harvesting nodes in fading wireless channels: Optimal policies," *IEEE J. Sel. Area. Comm.*, vol. 29, no. 8, pp. 1732–1743, Sept. 2011.
- [7] S. Bi, Y. Zeng, and R. Zhang, "Wireless powered communication networks: an overview," *IEEE Wireless Commun.*, vol. 23, no. 2, pp. 10–18, Apr. 2016.
- [8] L. Varshney, "Transporting information and energy simultaneously," in *Proc. 2008 IEEE Int. Symp. Inf. Theory*, pp. 1612–1616, July, 2008.
- [9] P. Grover and A. Sahai, "Shannon meets tesla: Wireless information and power transfer," in *Proc. 2010 IEEE Int. Symp. Inf. Theory*, pp. 2363–2367, Jun., 2010.
- [10] X. Lu, P. Wang, D. Niyato, D. I. Kim, and Z. Han, "Wireless networks with RF energy harvesting: A contemporary survey," *IEEE Commun. Surveys Tuts.*, vol. 17, no. 2, pp. 757–789, Nov. 2015.
- [11] S. Bi, C. K. Ho, and R. Zhang, "Wireless powered communication: opportunities and challenges," *IEEE Commun. Mag.*, vol. 53, no. 4, pp. 117–125, Apr. 2015.
- [12] D. Xu and Q. Li, "Joint power control and time allocation for wireless powered underlay cognitive radio networks," *to appear in IEEE Wireless Commun. Lett.*, 2017.
- [13] H. Ju and R. Zhang, "Throughput maximization in wireless powered communication networks," *IEEE Trans. Wireless Commun.*, vol. 13, no. 1, pp. 418–428, Jan. 2014.
- [14] K. Huang and V. K. N. Lau, "Enabling wireless power transfer in cellular networks: Architecture, modeling and deployment," *IEEE Transactions on Wireless Communications*, vol. 13, no. 2, pp. 902–912, Feb. 2014.
- [15] K. Huang and X. Zhou, "Cutting the last wires for mobile communications by microwave power transfer," *IEEE Commun. Mag.*, vol. 53, no. 6, pp. 86–93, Jun. 2015.
- [16] G. Chen, P. Xiao, J. R. Kelly, B. Li, and R. Tafazolli, "Full-duplex wireless-powered relay in two way cooperative networks," *IEEE Access*, vol. 5, pp. 1548–1558, Jan. 2017.
- [17] C. Zhong, G. Zheng, Z. Zhang, and G. K. Karagiannidis, "Optimum wirelessly powered relaying," *IEEE Signal Process. Lett.*, vol. 22, no. 10, pp. 1728–1732, Oct. 2015.
- [18] K. Chi, Y. H. Zhu, Y. Li, L. Huang, and M. Xia, "Minimization of transmission completion time in wireless powered communication networks," *to appear in IEEE Internet Things J.*, 2017.
- [19] K. W. Choi, L. Ginting, P. A. Rosyady, A. A. Aziz, and D. I. Kim, "Wireless-powered sensor networks: How to realize," *IEEE Trans. Wireless Commun.*, vol. 16, no. 1, pp. 221–234, Jan. 2017.
- [20] T. C. Hsu and Y. W. P. Hong, "Wireless power transfer for distributed estimation in wireless passive sensor networks," in *IEEE GlobalSIP, Orlando, FL, USA*, pp. 48–52, Dec. 2015.
- [21] V. V. Mai, W. Y. Shin, and K. Ishibashi, "Wireless power transfer for distributed estimation in sensor networks," *IEEE J. Sel. Topics Signal Process.*, vol. 11, pp. 549–562, April Apr. 2017.

- [22] H. Niu, B. Zhang, D. Guo, and M. Lu, "Robust secure design for relay wireless sensor networks with simultaneous wireless information and power transfer," *Int. J. Distrib. Sens. N.*, vol. 13, no. 6, Mar. 2017.
- [23] S. Boyd and L. Vandenberghe, *Convex Optimization*. Cambridge, UK: Cambridge University Press, 2004.
- [24] Y. Li, X. Qi, M. Keally, Z. Ren, G. Zhou, D. Xiao, and S. Deng, "Communication energy modeling and optimization through joint packet size analysis of BSN and WiFi networks," *IEEE Trans. Parallel Distrib. Syst.*, vol. 24, pp. 1741–1751, Sept 2013.
- [25] A. H. Mohsenian-Rad, V. W. S. Wong, J. Jatskevich, R. Schober, and A. Leon-Garcia, "Autonomous demand-side management based on game-theoretic energy consumption scheduling for the future smart grid," *IEEE Trans. Smart Grid*, vol. 1, no. 3, pp. 320–331, Dec. 2010.
- [26] M. Grant and S. Boyd, "CVX: Matlab software for disciplined convex programming." *Optimization Methods and Software*, Apr. 2012. <http://stanford.edu/~boyd/cvx>.
- [27] Y. Huang and D. P. Palomar, "Rank-constrained separable semidefinite programming with applications to optimal beamforming," *IEEE Trans. Signal Process.*, vol. 58, no. 2, pp. 664–678, Feb. 2010.